J Solid State Electrochem (2016) 20:993–1000
DOI 10.1007/s10008-015-3066-6

ORIGINAL PAPER

Oxidation of melatonin on a glassy carbon electrode modified with metallic glucosamines. Synthesis and characterization

Claudia A. Caro[1] · Luis Lillo[1] · Francisco J. Valenzuela[1] · Gerardo Cabello[1] · Erika Lang[2] · Diego Vallejos[1] · Cristóbal Castillo[1]

Received: 4 May 2015 / Revised: 23 October 2015 / Accepted: 27 October 2015 / Published online: 22 January 2016

Abstract In this study, a glassy carbon electrode modified with different cobalt glucosamines (CoGlu-R), iron glucosamines (FeGlu-R), and nickel glucosamines (NiGlu-R) was used for the electroanalytical determination of melatonin in buffer solutions at pH 7.3 using cyclic and square wave voltammetry. The complexes were synthesized and characterized by IR-TF, ^{1}H-NMR, and UV–visible spectroscopy. When comparing glucosamines of different metals, the influence of the nature of the metal on the activity is not very strong. The most active complex was CoGlu-R. The oxidation peak was used to determine melatonin in the concentration range of 10^{-8}–10^{-5} M with a detection limit of 2.15×10^{-7} M (LOD). Our results indicate that the current peak is under mass-transport control and probably suggest that chemical reactions coupled with electrochemical steps are involved. The melatonin oxidation current with this kind of modified electrodes is small but this modified electrode shows high selectivity in medium-199 (glutamine, phenol red, glucose, Na^{+}, CO_3^{2-}) with human placental tissue; trophoblast and endothelial cells (K^{+}, Ca^{2+}, traces of Cu^{2+} and Mg^{2+}), yet the tryptophan causes interference.

Keywords Melatonin · Glassy carbon electrode · Cyclic voltammetry · Metallic glucosamine

Introduction

Melatonin is a hormone produced mainly in the pineal gland and participates in neuro-endocrine and neuro-physiological processes ($C_{13}H_{16}N_2O_2$, 232.28 g/mol) [1, 2]. It plays a role in the biological clock and its dysfunction causes alterations [3]. Analytical techniques including capillary electrophoresis [4, 5], gas chromatography [6, 7], high-performance liquid chromatography (HPLC) [8–10], spectrofluorimetric–spectrophotometric [11, 12], and chemiluminescence [13] have been reported for the analysis of melatonin. Some of the above mentioned methods require a preliminary extraction and purification of melatonin and skilled personnel manipulating sophisticated instrumentation. Electrochemical methods are of great interest compared to other analytical techniques because of their simplicity and lower costs [14, 15]. To date, on the other hand, some electroanalytical methods have been reported for quantitative determination of melatonin [16–18]. Nevertheless, this approach is frequently limited by complications arising from the irreversible passivation of the electrode surface.

Today, the electroanalytical studies using biodegradable molecules are based principally on chitosan: first, in the determination of the substitution degree of modified chitosan by cyclic voltammetry [19], then in different films on glassy carbon (GCE) electrodes for the electrochemical determination of species like: azathioprine [20], 4-aminophenol, glucose oxidase, gluconobacteroxydans [21, 22], thiodicarb [23], mebendazole [24], glucose [25], and lysozyme [26] among other things. In this work, the problem with chitosan and its derivatives is that they present broad peaks and there is docking between the redox signals of metal and ligands [27, 28]. In this context, glassy

This paper is dedicated to Professor José H. Zagal on the occasion of his 65th birthday and in recognition of his outstanding contribution to electrochemistry.

✉ Claudia A. Caro
candkaro@hotmail.com

[1] Departamento de Ciencias Básicas, Facultad de Ciencias, Universidad del Bío-Bío, Campus Fernando May, Av. Andrés Bello s/n, Chillán, Chile

[2] CEM, Departamento de Biología, Facultad de Ciencias, Universidad de Chile, Santiago, Chile

carbon electrodes with chemical modifications of the monosaccharides allow obtaining molecules with novel properties for applications in industry and in biology. In the biomedical context, the selective chemical modifications are of interest in the drug development of slow liberation and derivatives with antioxidant, antitumor, and antimicrobial activity [29, 30]. The glucosamine ($C_6H_{13}NO_5$) is a very abundant amino sugar [31]. Recent studies have provided preliminary evidence that glucosamine may be bioavailable in the synovial fluid after oral administration [32]. This is a prominent precursor in the biochemical synthesis of glycosylated proteins and lipids. It is part of the structure of the polysaccharides chitosan and chitin, which compose the exoskeletons of crustaceans and other arthropods, cell walls in fungi, and many higher organisms. It is produced commercially by the hydrolysis of crustacean *exoskeletons* or less commonly by fermentation of a grain such as corn or wheat [31]. Interactions between mediator and active species can occur through certain functional groups. The complexes of Schiff bases derived from amino sugars with transition metals have been the focus of numerous studies with a view to their application in technology as catalyst [33–36] and in medicine [37, 38]. The properties of the complexes are related to the structure of ligands.

There are rather few studies of the interaction between glucosamine or its derivatives immobilized on different surfaces. Tominaga et al. studied the electrosynthesis of glucosamic acid from glucosamine at a gold electrode [39], whereas Sugawara et al. performed a voltammetric evaluation for the binding of glucosamine and wheat germ agglutinin [40]. The use of a biosensor amperometric sensor for glucose has been achieved using a hexacyanoferrate-chitosan oligomer mixture [41]. There are studies of coagulation characteristics of humic acid modified with glucosamine [42] and studies about its application in symptomatic primary knee osteoarthritis [43–48]. The anti-HIV-1 activity of glucosamine [49], bioactivity [50], anti-inflammatory [51, 52], antioxidant, and antimicrobial properties are also known [53, 54]. The use of glucosamine is expanding into different fields, even though the applications in electrochemistry are still low.

The aim of this study is to extend the use of glucosamine-type derivatives to selective sensors, specifically to the oxidation of melatonin. Thus, we report here, for the first time a study of glassy carbon electrodes modified with different metal complexes, to establish their selectivity for the detection of melatonin via its oxidation.

Experimental

Materials

Glucosamine, salicylaldehyde derivatives with different electron-donating and electron-withdrawing groups (5-bromine, 5-chlorine, 5-methoxy, 5-fluorine, 5-methyl, and 5-nitro), and $CoCl_2 \times H_2O$, $FeCl_2 \times H_2O$, and $NiCl_2 \times H_2O$ were obtained from Aldrich Chemical Co. and used for the synthesis of derivatives of cobalt, iron, copper, and nickel monomers. The analytical grade electrolytes (H_2SO_4, KCl, KH_2PO_3, and Na_2HPO_3) were obtained from Merck and used as provided. The solvents used for ^{1}H NMR spectroscopy were deuterium oxide 99.98 % and dimethyl sulfoxide-d_6 99.8 %, both of Merck.

Elemental analyses, FTIR, ^{1}H NMR spectroscopy, and UV–vis spectroscopy

The metal content was determined by atomic absorption using Perkin Elmer 2380 equipment. Elemental analyses were performed in a FISIONS-EA 1108 analyzer. The metallic glucosamine and derivatives were characterized by FTIR in a FTIR-4100 Jasco spectrophotometer. All spectra were recorded with an accumulation of 64 scans and resolution of 4 cm^{-1} from 4000 to 200 cm^{-1}. For IR spectra, the samples (100.0 mg) were dried for 24 h at 30 °C and were mechanically mixed with 20 mg of KBr. Derivation, including the Savitzky–Golay algorithm with 25 smoothing points, was performed using the OPUS/I.R: version 1.4 software incorporated into the hardware of the instrument [55, 56]. Proton nuclear magnetic resonance (^{1}H NMR) spectra were registered on a Bruker Avance DRX 400 spectrophotometer operating at 400.13 (^{1}H) MHz using DMSO-d_6 as solvent.

The UV–visible spectra of complexes were measured in phosphate buffer solution (pH = 7.3) and were obtained with 1 nm resolution in a Perkin Elmer Model Lambda 25 UV–vis spectrophotometer.

Electroanalytical measurements

The working electrode was a glassy carbon disk electrode from Pine Instruments of exposing a 0.196 cm^2 geometrical area mounted in Teflon. Before each experiment, the electrode was polished with 1200 and 4000 grit emery paper followed by ultrasonic cleaning in ultra-pure Milli-Q water. A saturated calomel electrode (SCE) was used as reference and the auxiliary electrode was a platinum (99.99 %, Pine Instruments) spiral wire exposing an area of 14 cm^2. The electrolytes were prepared from deionized, double-distilled water.

Complexes were adsorbed on glassy carbon by placing a drop of a 1.5×10^{-3} M of the monomer in a phosphate buffer solution (pH = 7.3) on the electrode surface for 20 min. After this, the excess of complex was removed with H_2O followed by rinsing with ethanol [57]. Dioxygen was eliminated by purging solutions with nitrogen for 25 min. Melatonin introduction into the electrochemical cell was done by adding aliquots of 10 μL of a 2.153×10^{-4} M melatonin solution. Electrochemical measurements were conducted in phosphate buffer solution (pH = 7.3) and with an Electrochemical

Analyzer potentiostat/galvanostat Model 600 D Series of CH Instruments.

Synthesis of glucosamine–M(II) complexes

The Schiff bases were synthesized by reaction of D-cloro-glucosamine (0.1 g, 9.01×10^{-5} mM) with salicylaldehyde derivatives in 15 mL of NaOH 0.5 M (in methanol) for 5 min. The solvent was evaporated at 176 mbar, 60 rpm, at 40 °C for 30 min and the remaining solid was washed with distilled water and dried [58].

The salicylaldehyde derivatives are the following: 2-hydroxy-5-methoxybenzaldehyde ($R = -OCH_3$), 5-hydroxy-5-nitrobenzaldehyde ($R = -NO_2$), 5-hydroxy-5-methylbenzaldehyde ($R = -CH_3$), 5-hydroxy-5-chlorobenzaldehyde ($R = -Cl$), 5-hydroxy-5-fluorobenzaldehyde ($R = -F$), and 5-hydroxy-5-bromobenzaldehyde ($R = -Br$).

Glucosamine–M(II) complexes were prepared by mixing Schiff base powders (0.050 g) with $FeCl_2$, $CoCl_2$, and $NiCl_2$ (0.022 g) solutions. These mixtures were refluxed in methanol with stirring for 16 h at 60 °C. The solvent was evaporated at 176 mbar, 60 rpm, at 40 °C for 30 min. The crystals were filtered off, and the filtrated solution was concentrated under vacuum. The resulting solids were washed with methanol and ethyl ether finally [27, 58].

Results and discussion

Elemental analyses, FTIR, and ^{1}H NMR spectroscopy

The elemental analysis results of the Schiff bases and the content of metal in the complexes proved that the reaction gives bidentate, mononuclear metal (II) complexes [58]. The most significant bands found in the FTIR spectra of Schiff bases and glucosamine-complexes of the Schiff bases are present (see Table 1). The FTIR spectra of Schiff bases showed high absorption levels between 1628.96 and 1675.84 cm^{-1} attributed to the C=N stretching characteristic of the imino group. The second derivative FTIR spectra of glucosamine complexes of the Schiff bases showed a tendency to lower wavenumbers in the C=N absorption relative to the free ligand spectrum, indicating the coordination of the nitrogen atom of the Schiff bases to the metal ion [59]. Two bands, in relation to the free ligand, in the second derivative spectrum assigned to M-O (390–400 cm^{-1}) and to M-N (270–280 cm^{-1}) stretching vibrations corroborates the formation of the M(II) complex [57].

The spectral features suggest that the alcoholic groups of the monosaccharide moiety do not participate in the coordination to the metal.

The ^{1}H NMR spectrum of the Schiff base in DMSO-d_6 obtained by reaction of D-glucosamine with *o*-salicylaldehyde showed at low field, the signal assigned to the imino proton that appears as two singlets at 7.671 and 7.516 ppm and two singlets at 10.244 and 10.735 ppm assigned to the glucosamine hydroxyl proton (Fig. 1a).

The ^{1}H NMR spectra of the different D-glucosamine metal complexes reveal the presence of Fe(II), Ni(II), and Co(II) (when $R = -H$). The spectrum of the iron D-glucosamine complex is shown in Fig. 1b, for example. They present lower field shifts of the imine proton when compared to the same proton in the Schiff base of D-glucosamine. The Fe(II) complex shows the imine proton signal as two singlets at 10.754 and 10.252 ppm (Co(II) complex has a similar behavior). The Ni(II) complex shows the imine proton signal as two singlets but the lower field shifts is not so pronounced (~9 and 10 ppm). The ^{1}H NMR spectra of many Ni(II) complexes with Schiff bases derived from aliphatic amines have shown great variations in the chemical shifts of the protons compared to the free imine due to the planar diamagnetic-tetrahedral paramagnetic equilibria. The small paramagnetic shifts in the NMR spectra of the Ni(II) complex are indicative of a small proportion of non-planar species in DMSO solutions [60].

Table 1 IR bands of imino group of the Schiff bases and of the complexes

Infrared (cm^{-1})									
Sample	Base ν_{C-N} (imine)	M=Co ν_{C-N} (imine)	M=Fe ν_{C-N} (imine)	M=Cu ν_{C-N} (imine)	M=Ni ν_{C-N} (imine)	C-O-C	OH radical	=C-H	C=C
MGlu-H	1675.12	1620.15	1608.33	1664.27	1664.59	1150.33		3060.48	
MGlu-Br	1671.97	1669.09	1669.95			1153.22		3067.23	
MGlu-Cl	1688.39	1626.66	1680.58			1152.26	3416.28	3046.98	
MGlu-F	1688.39	1386.3	1659.45				3259.11	3059.51	
MGlu-CH_3	1628.96	1623.77	1598.7	1627.03	1618.35	1159.27		3062.41	1590.99
MGlu-NO_2	1661.86	1656.55	1606.42	1661.86		1145.51	3204.15	3068.19	
MGlu-OCH_3	1641.96	1637.11	1603.52			1162.82	3484.46	2926.45	1590.99

ν; stretching base; glucosamine-salicylaldehyde

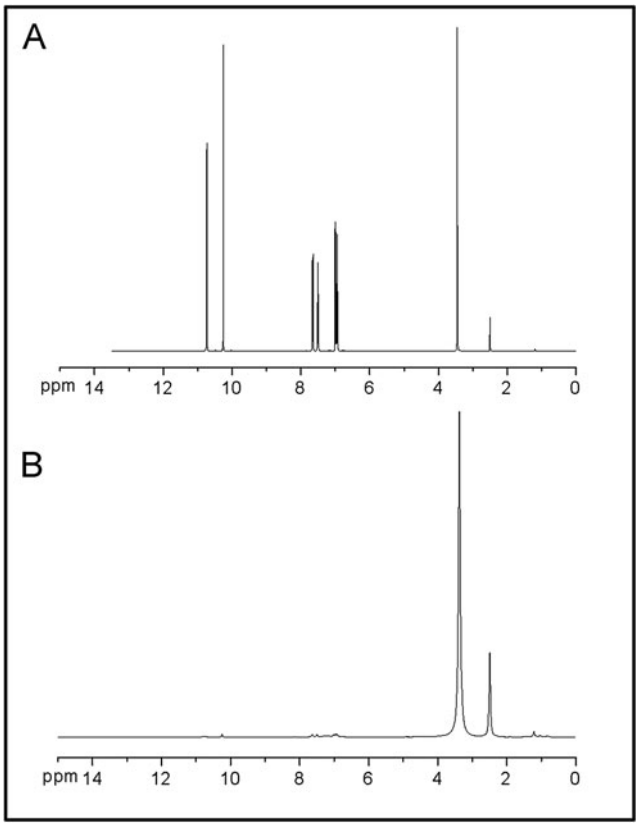

Fig. 1 ^{1}H NMR spectrum in DMSO-d_6 of (**a**) Schiff base obtained by reaction of D-glucosamine with *o*-salicylaldehyde and (**b**) iron glucosamine complex. 400 MHz, 25 °C

Results found in the ^{1}H NMR spectrum indicate that the imino group participates in the complexation with the metal and the participation of the hydroxyl groups of the sugar residues might be excluded.

UV–vis spectroscopy

The absorption spectra of glucosamine-M(II) complexes dissolved in phosphate buffer solution (pH = 7.3) is shown in Fig. 2. All transitions below 400 nm are assigned to intraligand charge transfer, attributed to the benzene ring transition ($\pi \rightarrow \pi^*$) at lower wavelength, and the second transition was assigned to the -C_6H_5-OH group ($n \rightarrow \pi^*$) [27]. For all glucosamine-Fe(II) complexes, the electronic transitions appear shifted to higher energies compared with Schiff bases (Fig. 2a) and all complexes exhibit signals attributed to d-d transitions.

For all glucosamine-Co(II) complexes, the electronic transitions move to lower energies except when $R = -$Cl and −Br. For some complexes, new signals appear when compared to Schiff bases [27]. For example when $R = -$H, a new signal appears at 375 nm (Fig. 2b).

The absorption spectra of glucosamine-Ni(II) complexes dissolved in phosphate buffer solution are shown in Fig. 2c. For all complexes, the electronic transitions shift to lower energies. Only for glucosamine-Co(II) complexes, new signals appear indicating the formation of an intermediate before melatonin oxidation (see Fig. 3).

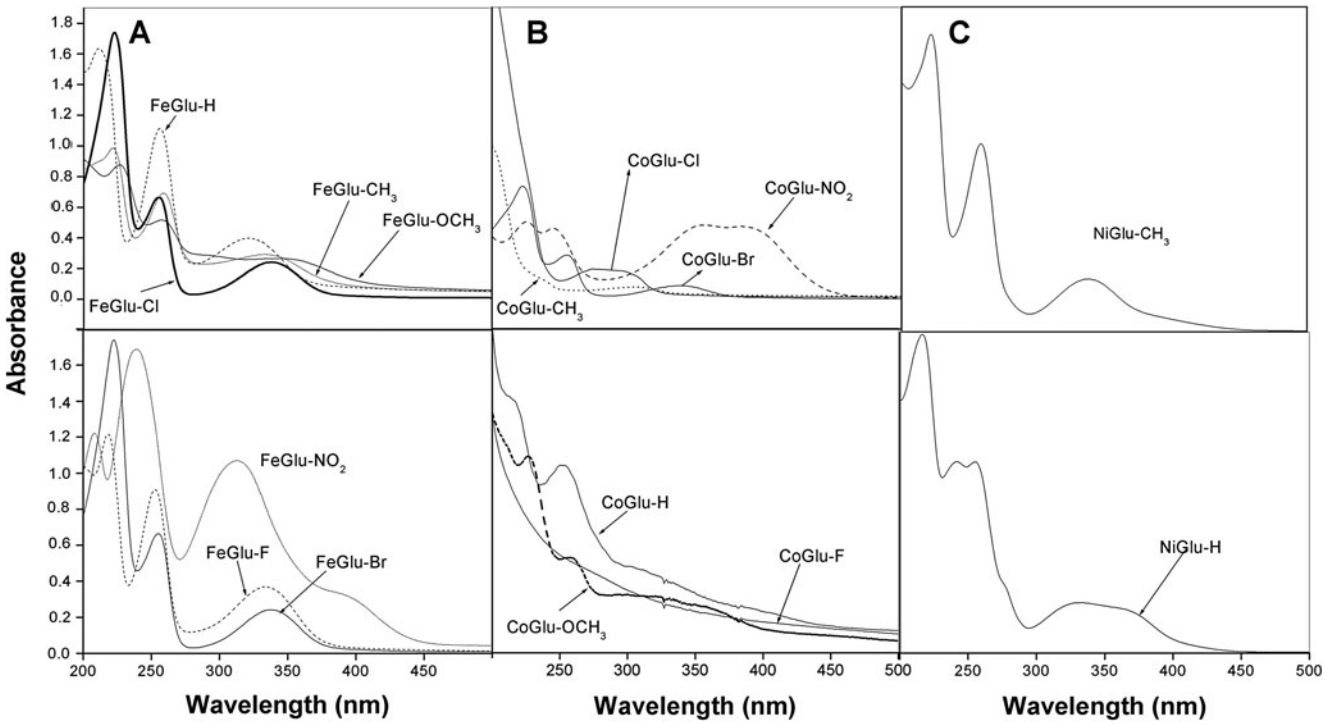

Fig. 2 UV–visible spectra of the following complexes. (**a**) Iron glucosamine complexes. (**b**) Cobalt glucosamine complexes. (**c**) Nickel glucosamine complexes. Phosphate buffer pH 7.3

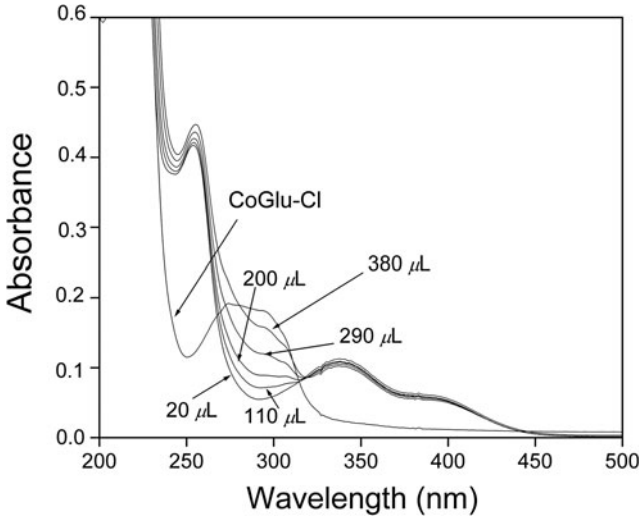

Fig. 3 UV–visible spectra of cobalt glucosamine-Cl in phosphate buffer pH 7.3: (1) without and with melatonin, (2) 2.15×10^{-7} M, (3) 1.18×10^{-6} M, (4) 2.15×10^{-6} M, (5) 3.12×10^{-7} M, (6) 4.09×10^{-6} M

Electrochemical studies

Figure 4 depicts a series of cyclic voltammograms illustrating the potentiodynamic response of different substituted glucosamine-M(II) complexes adsorbed on GCE. Cyclic voltammograms were obtained in KH_2PO_4-Na_2HPO_4 buffer (pH = 7.26). Intrinsic parameters of the redox couple or redox peak of the adsorbed catalyst were determined using cyclic voltammetry (scan rates up to 0.1 V/s) and differential pulse voltammetry. The glucosamine-Co(II) complexes show one redox couple that corresponds to processes centered on the metal and involving the Co(III)/(II) couple [24]. For example, the glucosamine-Co(II) complex (Fig. 4a) when $R = -H$ shows an almost reversible redox couple at ca. −0.117 V (anodic)/−0.123 V (cathodic) attributed to the Co(III)/(II) redox process. Similar processes are observed for the glucosamine-Co(II) complexes when $R = -Br$, −Cl, and −F with signals at ca. 0.094/−0.008 V, 0.089/−0.041 V, and 0.109/0.053 V, respectively, for the corresponding anodic/cathodic peaks.

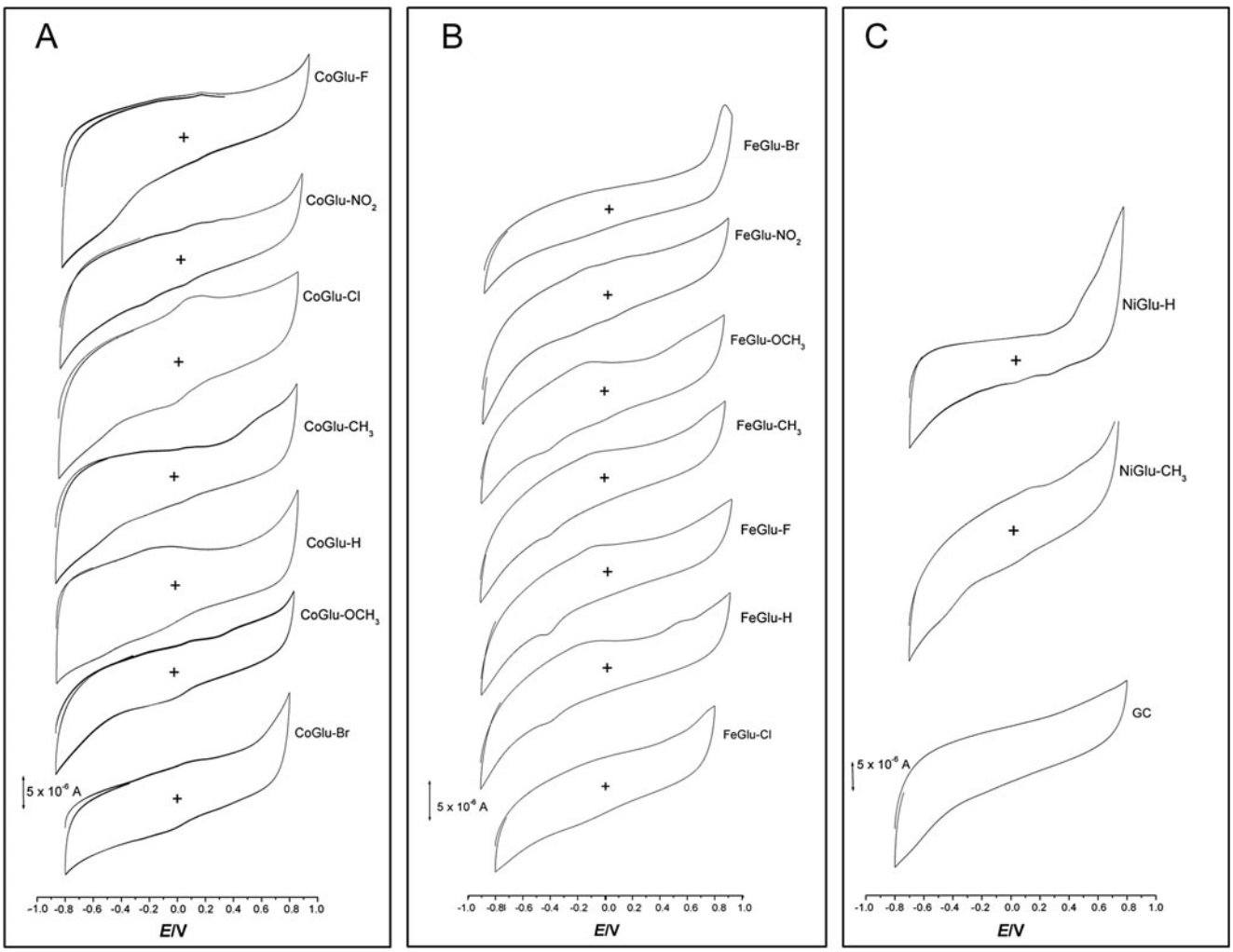

Fig. 4 Cyclic voltammograms of (**a**) cobalt glucosamine complexes on glassy carbon surface, (**b**) iron glucosamine complexes on glassy carbon surface, (**c**) nickel glucosamine complexes on glassy carbon surface. Phosphate buffer pH 7.3, N_2 saturated. Scan rate, 0.1 Vs^{-1} vs. SCE

When $R=-CH_3$, an irreversible weak signal was observed with an anodic peak at 0.087 and a cathodic peak at −0.094 V. When $R=-OCH_3$, an anodic peak appears at 0.415 V and an irreversible redox process with an anodic peak at 0.121 V and a cathodic peak at −0.043 V. The glucosamine-Co(II) when $R=-NO_2$ presents two redox couples at ca. 0.102/0.017 V and −0.209/−0.232 V. Similar patterns are observed in cyclic voltammograms of glucosamine-Fe(II) complexes and cyclic voltammogram glucosamine-Co(II) (Fig. 4b). All glucosamine-Fe(II) complexes, excluding those where $R=-Cl$ and −Br present a redox couple. When $R=-OCH_3$, −F, this couple appears at ca. −0.357 (cathodic peak) and −0.102 V (anodic peak), for the complex substituted with CH_3 group, the couple appears at −0.335 V (cathodic peak) and −0.064 V (anodic peak). Similar processes present the complex when $R=-H$ at −0.351/-0.127 and other irreversible signal at 0.475 V, while when $R=-NO_2$, peaks are observed at 0.129/0.023 and −0.116/−0.191 V.

The glucosamine-Ni(II) complexes exhibit an irreversible redox couple; for $R=-CH_3$, the couple appears at 0.003/0.164 V and when $R=-H$ at −0.314/0.645 V.

The cyclic voltammograms obtained on the glassy carbon electrode modified with adsorbed Co, Fe, and Ni glucosamine complexes for the oxidation of melatonin show an anodic peak at ca. 0.6 V. If the rates as currents for melatonin oxidation are compared at constant potential for the different metal complexes, the trend in activity is as follows: CoGlu-R > FeGlu-R > NiGlu-R. The high activity of CoGlu-R seems to be related to the connection between CoGlu-R and melatonin observed in the UV–vis spectra. The higher activity of Co and Fe complexes compared to Ni is probably a reflection that Co and Fe chelates have almost half-filled d orbitals and have a higher tendency to bind extraplanar ligands (in this case melatonin) than Ni(II) complexes.

In order to get further insight on this behavior, we have explored the activity of various Co and Fe complexes bearing different substituents. The trend in reactivity for CoGlu-R is as follows: CoGlu-Cl > CoGlu-H > CoGlu-CH_3 > CoGlu-Br > CoGlu-NO_2 > CoGlu-F > CoGlu-OCH_3. CoGlu-Cl is the most active complex. For FeGlu-R, it was as follows: FeGlu-Cl > FeGlu-OCH_3 > FeGlu-Br > FeGlu-NO_2 = FeGlu-F > FeGlu-CH_3 > FeGlu-H. There is not a correlation between the peak current and Hammett parameters of substituent, then, the redox potential of the complex does not contribute to the driving force of the reaction.

Figure 5a shows the square wave voltammograms obtained on the glassy carbon electrode modified with adsorbed CoGlu-Br for the oxidation of melatonin, with concentrations ranging from 10^{-8} to 10^{-5} M, where the limit of detection (LOD) is 2.15×10^{-7} M. An anodic oxidation peak is observed at ca. 0.6 V, and its intensity is directly proportional to the concentration of melatonin (see Fig. 5b) and its potential shifts towards positive values by increasing melatonin concentration.

Figure 6 illustrates as a typical example, a series of cyclic voltammograms obtained at different potential scan rates with CoGlu-Cl adsorbed on the glassy carbon electrode, for a given melatonin concentration. Analysis of these data shows that the peak currents I_p are proportional to the square root of potential scan rate $v^{1/2}$ (Fig. 6a), indicating that the current peak is under mass-transport control, (ii) the peak potential E_p shifts with scan rate (as log v) (Fig. 6b), indicating the kinetic irreversibility of the melatonin electrocatalytic oxidation process and probably suggest that chemical reactions coupled with electrochemical steps are involved, and (iii) the variation of the ratio $I_p/v^{1/2}$ versus v shows the typical evolution expected for a catalytic process [61]. This was observed for all the examined glucosamines.

Probably, the mechanism for the most active complex (CoGlu-Cl) can also be explained according to the following scheme:

$$\mathrm{M(III)Glu\text{-}R + RNH \rightarrow [RNH\text{-}M(III)Glu\text{-}R]}$$
$$\mathrm{[RNH\text{-}M(III)Glu\text{-}R] \rightarrow [RNH\text{-}M(III)Glu\text{-}R]^+ + e}$$
$$\mathrm{[RNH\text{-}M(III)Glu\text{-}R]^+ \rightarrow [RN\bullet\text{-}M(III)Glu\text{-}R]^+ + e + H^+}$$
$$\mathrm{2[RN\bullet\text{-}M(III)Glu\text{-}R]^+ \rightarrow 2M(III)Glu\text{-}R + RN\text{-}NR + 2H^+}$$

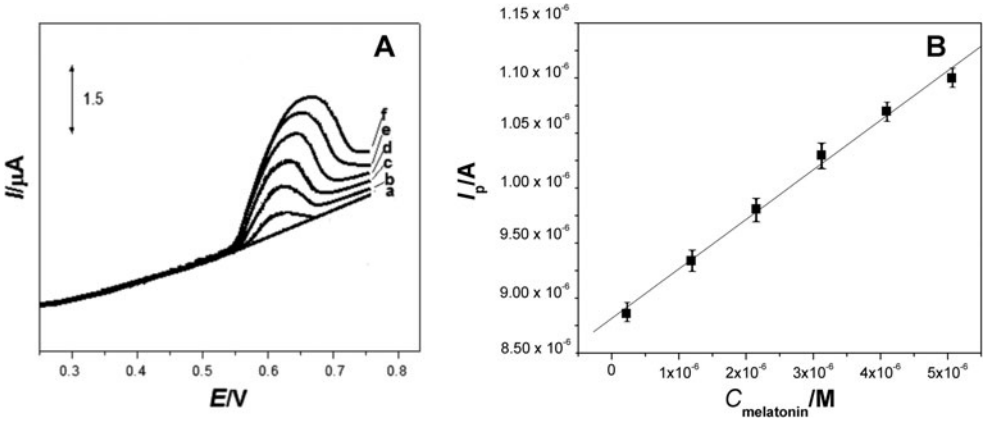

Fig. 5 **a** Square wave voltammograms at 100 mV/s obtained on the glassy carbon electrode modified with adsorbed CoGlu-Br for the oxidation of melatonin, with concentrations ranging from 2.15×10^{-7} to 5.06×10^{-5} M in phosphate buffer pH 7.3, N_2 saturated **b** peak current I_p vs. concentration of melatonin $C_{melatonin}$

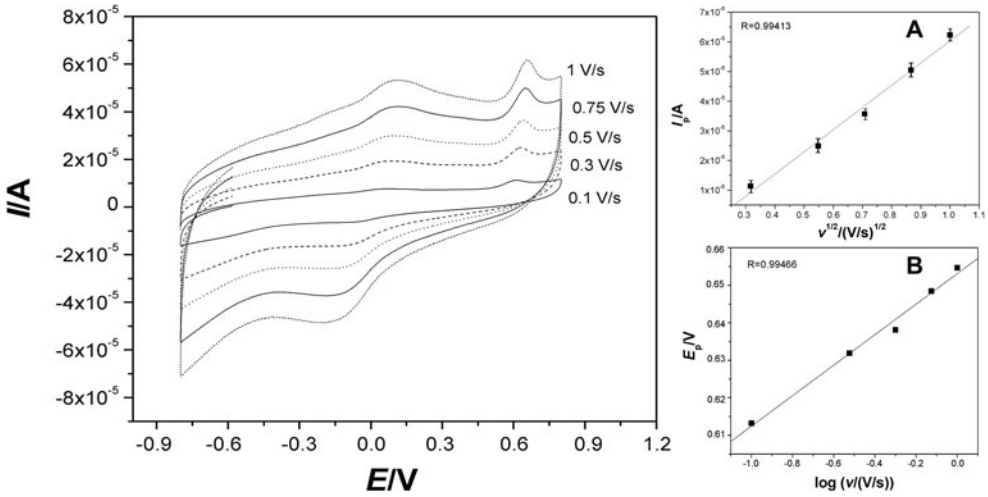

Fig. 6 Cyclic voltammograms obtained at different potential scan rates with CoGlu-Cl adsorbed on the glassy carbon electrode, for 3.12×10^{-6} M of melatonin. **a** The peak currents I_p vs. square root of scan rate $v^{1/2}$ **b** peak potential E_p vs. logarithm of scan rate log v

The LOD in this work was lower than the observed in the same conditions, however there are publications with LOD of 1×10^{-8} M at pH 5 (work electrode of mercury) [17] and 1×10^{-11} M [16] in $HClO_4$. The catalytic activity of these complexes for the oxidation of melatonin is compensated with its high selectivity. Figure 7 shows two cyclic voltammograms obtained with CoGlu-Cl adsorbed on the glassy carbon electrode, for a given melatonin concentration in buffer solution and for the same melatonin concentration in medium-199 (glutamine, phenol red, glucose, Na^+, CO_3^{2-}) with human placental tissue of patient without medicine; trophoblast and endothelial cells (K^+, Ca^{2+}, 20 amino acids, and traces of Cu^{2+} and Mg^{2+}). When a tryptophan solution was added, the voltammogram showed that its oxidation potential is close to that of melatonin and thus affects the oxidation peak current of melatonin. This was solved with square wave voltammetry.

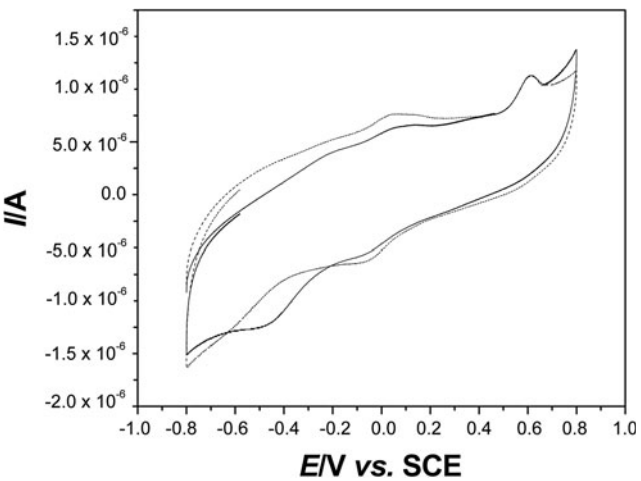

Fig. 7 Cyclic voltammograms obtained on the glassy carbon electrode modified with adsorbed CoGlu-Cl for (——) the oxidation of melatonin in phosphate buffer (pH = 7.3), and (—) for the oxidation of melatonin in phosphate buffer with amino acids, sugar, and human tissue. 100 mV/s, melatonin 3.12×10^{-6} M

Conclusions

Modified glassy carbon electrodes with iron, cobalt, and nickel glucosamine complexes were used for melatonin determination in sample pretreatment and solution with amino acids, sugar, and human tissue. We have reported the preparation of glucosamine complexes by the reaction of Schiff bases with different metals (M = Fe, Co, and Ni). The glucosamine complexes were characterized by FTIR, ^{1}H NMR spectroscopy, UV–vis spectrophotometry, and cyclic voltammetry.

In general, metallic glucosamines exhibit low catalytic activity for the oxidation of melatonin at pH 7.3. When comparing glucosamines of different metals, the influence of the nature of the metal on the activity is not strong but the detection limit in a sample with amino acids, sugar, and human tissue was of 2.15×10^{-7} M (0.05 g/mL). The most active complex is CoGlu-Cl, and the effect of substituents on the periphery of the salicylaldehyde ligand is not pronounced due to the fact that charge transfer is not the rate-determining step in the melatonin oxidation process. The groups cause a shift of the UV–vis bands to lower energies for iron, nickel, glucosamines, and for cobalt complexes, the bands shift to higher energies and form an intermediary between cobalt and melatonin before the melatonin oxidation. These complexes present high selectivity for the oxidation of melatonin (for a specific patient) but with higher concentration of tryptophan in the solution, the interference was serious.

Acknowledgments The authors are grateful to the financial support from FONDECYT Projects No. 1120164 and to Dirección de Investigación de la Universidad del Bío-Bío (Grant DIUBB 142209 4/R).

References

1. Mayo JC, Sainz RM, Tan DX, Antolin I, Rodriguez C, Reiter RJ (2005) Endocrine 27:169–178

2. Reiter RJ (1991) Endocrinol Rev 12:151–180
3. Reppert SM, Weaver DR, Rivkees SA, Stopa EG (1988) Science 242:78–81
4. Cartoni GP, Coccioli F, Jasionowska R, Masci M (2000) Chromatographia 52:603–606
5. Chen G, Ding X, Cao Z, Ye J (2000) Anal Chim Acta 408:249–256
6. Aboul-Enein HY, Doneau C, Covaci A (1999) Biomed Chromatogr 13:24–26
7. Nunez-Vergara LJ, Squella JA, Sturm JC, Baez H, Camargo C (2001) J Pharm Biomed Anal 26:929–938
8. Munoz LPJ, Ceinos MR, Soengas LJ, Míguez MJ (2009) J Chromatogr B 877:2173–2177
9. Rosanna MW, Chaua BA (2009) Biomed Chromatogr 23:175–181
10. Varvaresou A, Tsirivas E, Iakovou K, Gikas E, Papathomas Z, Vonaparti A, Panderi I (2006) Anal Chim Acta 573–574:284–290
11. Asadpour-Zeynali K, Bastami M (2010) Spectrochim Acta A 75: 589–597
12. Sorouraddin MH, Rashidi MR, Ghorbani-Kalhor E, Asadpour-Zeynali K (2005) II Farmaco 60:451–458
13. Lu J, Lau C, Lee MK, Kai M (2002) Anal Chim Acta 455:193–198
14. Levent A, Yardim Y, Zentürk Z (2009) Electrochim Acta 55:190–195
15. Wang SJ, Liaw HW, Tsai YC (2009) Electrochem Commun 11: 733–735
16. Corujo-Antuna JL, Abad-Villar EM, Fernandez-Abedul MT, Costa-Garcıa A (2003) J Pharm Biomed Anal 31:421–429
17. Beltagi AM, Khashaba PY, Ghoneim MM (2003) Electroanalysis 15:1121–1128
18. Qu W, Wang F, Dafu Cui SH (2005) Microchim Acta 150:109–114
19. Aldana AA, Strumia MC, Yudi LM, Martinelli M, Juarez AV (2014) Electrochim Acta 117:534–540
20. Shahrokhian S, Ghalkhani M (2010) Electrochim Acta 55(11): 3621–3627
21. Yin H, Ma Q, Zhou Y, Ai S, Zhu L (2010) Electrochim Acta 55(23): 7102–7108
22. Yılmaz Ö, Demirkol DO, Gülcemal S, Kılınç A, Timur S, Çetinkaya B (2012) Colloids Surf B 100:62–68
23. De Lima F, Lucca BG, Barbosa AMJ, Ferreira VS, Moccelini SK, Franzoi AC (2010) Enzym Microb Technol 47(4):153–158
24. De Lima F, Lucca BG, Barbosa AMJ, Ferreira VS, Moccelini SK, Franzoi AC, Vieira IC, Ghalkhani M, Shahrokhian S (2013) Sensors Actuators B 185:669–674
25. Singh J, Khanra P, Kuila T, Srivastava M, Das AK, Kim NH, Jung BJ, Kim DY, Lee SH, Lee DW, Kim D-G, Lee JH (2013) Process Biochem 48(11):1724–1735
26. Erdem A, Eksin E, Muti M (2014) Colloids Surf B 115:205–211
27. Caro CA, Cabello G, Landaeta E, Pérez J, Zagal JH, Lillo L (2013) Russ J Appl Chem 86:1791–1797
28. Caro CA, Cabello G, Landaeta E, Pérez J, González M, Zagal JH, Lillo L (2014) J Coord Chem 67:4114–4124
29. Wang X, Liu B, Li X, Sun R (2012) Nanotechnology 23(49): 495706
30. Stokes SS, Albert R, Buurman ET, Andrews B, Shapiro AB, Green OM, McKenzie AR, Otterbein LR (2012) Bioorg Med Chem Lett 22(23):7019–7023
31. Pigman WW, Horton D, Wander JD (1980) The Carbohydrates, vol. IB. Academic Press, New York
32. Kawcak CE, McIlwraith CW, Equine J (2011) Vet Sci 31(4): 155–159
33. Diéguez M, Pàmies O, Ruiz A, Díaz Y, Castillón S, Claver C (2004) Coord Chem Rev 248:2165–2192
34. Borriello C, Del Litto R, Panunzi A, Ruffo F (2004) Tetrahedron Asymmetry 15(4):681–686
35. Chatterjee D, Basak S, Mitra A, Sengupta A, Le Bras J, Muzart J (2006) Inorg Chim Acta 359:1325–1328
36. Chatterjee D, Basak S, Riahi A, Muzart J (2006) J Mol Catal A Chem 255:283–289
37. Ying F, Yi L, Changli X, Songsheg Q, Zhifeng L, Haoyu S, Maosheng D, Xiangcai Z (1996) Thermochim Acta 285:181–189
38. Bayly SR, Fisher CL, Storr T, Adam MJ, Orvig C (2004) Bioconjug Chem 15:923–926
39. Tominaga M, Nagashima M, Taniguchi I (2007) Electrochem Commun 9(5):911–914
40. Sugawara K, Kamiya N, Hirabayashi G, Kuramitz H (2007) Talanta 72(3):1123–1128
41. Lee S-H, Fang H-Y, Chen W-C (2006) Sensors Actuators B 117(1): 236–243
42. Terashima M, Tanaka S, Fukushima M (2007) Chemosphere 69(2): 240–246
43. Bottegoni C, Muzzarelli RAA, Giovannini F, Busilacchi A, Gigante A (2014) Carbohydr Polym 109:126–138
44. Shahine EM, Elhadidi AS (2014) Alex J Med 50(2):159–163
45. Henrotin Y, Marty M, Mobasheri A (2014) Maturitas 78(3):184–187
46. Su N, Yang X, Liu Y, Huang Y, Shi Z (2014) J Cranio-Maxillofac Surg 42(6):846–851
47. Onigbinde AT, Talabi AE, Shehu RA (2011) Hong Kong Physiother J 29(2):79–85
48. Yang J, Li J-R, Yang J-X, Li L-L, Ouyang W-J, Wu S-W, Zhang F (2014) Chin Chem Lett 25(7):1052–1056
49. Hong PK, Gottardi D, Ndagijimana M, Betti M (2014) Food Chem 142:285–293
50. Shin J-A, Hwang J-S, Kim S-Y, Oh S-K, Nam G, Han I-O (2013) Neurosci Lett 550:162–167
51. Wu Y-L, Lin A-H, Chen C-H, Huang W-C, Wang H-Y, Liu M-H, Lee T-S, Kou YR (2014) Free Radic Biol Med 69:208–218
52. Jamialahmadi K, Arasteh O, Matbou Riahi M, Mehri S, Riahi-Zanjani B, Karimi G (2014) Environ Toxicol Pharmacol 38(1): 212–219
53. Gottardi D, Hong PK, Ndagijimana M, Betti M (2014) Food Sci Technol-LEB 57(1):181–187
54. Costamagna J, Lillo LE, Matsuhiro B, Noseda MD, Villagran M (2003) Carbohydr Res 338:1535
55. Da Silva CM, da Silva DL, Modolo LV, Alves RB, de Resende MA, Martins CVB, de Fatima A (2011) J Adv Res 2:1–8
56. Caro C, Bedioui F, Páez M, Cárdenas-Jirón G, Zagal JH (2004) J Electrochem Soc 151:E32–E39
57. Costamagna J, Lillo L, Matsuhiro B, Noseda M, Villagrán M (2003) Carbohydr Res 338:1535–1542
58. Costamagna J, Barroso NP, Matsuhiro B, Villagran M (1998) Inorg Chim Acta 273:191–195
59. Caro C, Bedioui F, Zagal JH (2002) Electrochim Acta 47:1489–1494
60. Costamagna J, Vargas J, Latorre R, Alvarado A, Mena G (1992) Coord Chem Rev 119:67–85
61. Southampton Electrochem Group (1985) Instrumental Methods in Electrochemistry. Ellis Horwood, England